HHS Public Access

Author manuscript

J Immunol. Author manuscript; available in PMC 2015 October 30.

Published in final edited form as:

J Immunol. 1995 January 1; 154(1): 226–238.

A Human Anti-Insulin IgG Autoantibody Apparently Arises Through Clonal Selection from an Insulin-Specific "Germ-Line" Natural Antibody Template:

Analysis by V Gene Segment Reassortment and Site-Directed Mutagenesis[1]

Yuji Ichiyoshi[*,2], **Min Zhou**[†], and **Paolo Casali**[3,*]

[*]Division of Molecular Immunology, Department of Pathology, Cornell University Medical College, New York, NY 10021

[†]Department of Pharmacology, New York University School of Medicine, New York, NY 10016

Abstract

We analyzed the structural correlates underlying the insulin-dependent selection of the specific anti-insulin IgG1 κ mAb13-producing cell clone, derived from a patient with insulin-dependent diabetes mellitus treated with recombinant human insulin. First, we cloned the germ-line genes that putatively gave rise to the expressed V_H and Vκ segments and used them to generate the full (unmutated) "germ-line revertant" of the "wild-type" (somatically mutated) mAb13, using recombinant PCR methods and an in vitro human Cγ1 and Cκ expression system. The full "germ-line revertant" bound insulin specifically and in a dose-saturable fashion, but with a relative avidity (Av_{rel}) more than three-fold lower than that of its wild-type counterpart (Av_{rel}, 1.69×10^{-8} vs 4.91×10^{-9} g/μl). Second, we established, by reassorting wild-type and germ-line revertant forms of the mAb13 V_H and Vκ segments, that the increased Av_{rel} for insulin of mAb13 when compared with its full "germ-line revertant" counterpart was entirely dependent on the mutations in the V_H not those in the Vκ chain. Third, we determined, by site-directed mutagenesis experiments, that of the three mutations in the mAb13 V_H segment (Ser→Gly, Ser→Thr, and Ser→Arg at positions 31, 56, and 58, respectively), only Arg58 was crucial in increasing the mAb13 Av_{rel} (from 1.44×10^{-8} to 5.14×10^{-9} g/μl) and affinity (K_d, from 189 to 59 nM) for insulin. The affinity enhancement mediated by the V_H segment Arg58 residue reflected about a threefold decrease in dissociation rate constant (K_{off}, from 4.92×10^{-3} to 1.54×10^{-3} s^{-1})but not an increase in association rate constant (K_{on}, from 2.60×10^4 to 2.61×10^4 M^{-1} s^{-1}), and it contrasted with the complete loss of insulin binding resulting from the substitution of the V_H segment Asn52 by Lys. The present findings suggest that human insulin, a self Ag, has the potential to recruit a natural autoantibody-producing cell precursor expressing a specific surface receptor for Ag in unmutated configuration, and drive it through affinity maturation. They also show that binding of insulin by such a receptor can be enhanced or completely abrogated by a single amino acid change.

[1]This work was supported by the U.S. Public Health Service Grant AR-40908. This is publication 1 from the Division of Molecular Immunology.

[3]Address correspondence and reprint requests to: Dr. Paolo Casali, Division of Molecular Immunology, Department of Pathology, Cornell University Medical College, 1300 York Avenue, New York, NY 10021.

[2]Present address: Department of General Medicine, Kyushu University Hospital, Fukuoka 812, Japan.

Some human autoimmune disease-related autoantibodies, such as anti-DNA Abs in SLE patients (1–4) and rheumatoid factors (RF) in rheumatoid arthritis patients (5–8), display point-mutations in the V_H and V_L segments that are consistent in nature and distribution with clonal selection by Ags. However, the structural features and the specificity and high affinity of these autoantibodies for the relevant self Ag do not necessarily point at the self Ags themselves as instrumental in the clonal selection process. The ability of self Ag to induce affinity maturation in autoantibodies has been questioned, and it has been suggested that autoantibodies might be selected by unrelated cross-reacting perhaps foreign Ags, such as those on microbial agents (reviewed in 9, 10). A stronger evidence for selection by self Ag of an autoantibody-producing cell precursor would entail the demonstration that the germ-line template Ig progenitor of the somatically mutated autoantibody is capable of specifically binding the relevant self Ag, and that some of the point mutations observed in the "affinity mature" autoantibody are crucial in enhancing this binding.

The administration of recombinant human insulin for therapeutic purposes provides a unique opportunity for the structural analysis of specific autoantibodies actually induced by a self Ag, to which naturally occurring Abs exist in the normal B cell repertoire (10–12). Recently, we have reported the complete V_H and Vκ gene sequences of human-specific anti-insulin IgG autoantibodies derived from patients with insulin-dependent diabetes mellitus (IDDM)[4] treated with human recombinant insulin (12, 13). When compared with those of the closest germ-line genes, the IgG mAb Ig V_H and Vκ genes displayed a number of differences that are consistent in nature and distribution with those resulting from an Ag-driven clonal selection (13). In one IgG mAb, designated mAb13, these nucleotide differences were formally proved to represent somatic point-mutations by differentially targeted PCR amplification and Southern blot hybridization of the genomic DNA from the mAb13-producing cell line and autologous PMN (13). The higher and lower numbers of amino acid replacement (R) mutations in the V_H segment CDRs and FRs, respectively, than those expected by chance alone, were consistent with exertion of a positive antigenic pressure to mutate the structure of the CDRs and to preserve that of the FRs (14–17).

To analyze the structural correlates underlying the insulin-dependent emergence of the specific anti-insulin mAb13-producing cell clone, we constructed the germ-line revertants of the somatically mutated anti-insulin IgG mAb13 V_H and Vκ genes, and analyzed the Ag-binding activity of the gene products. The full germ-line revertant of mAb13 bound specifically to insulin, although with lower affinity than that of the wild-type mAb13. In addition, we analyzed the affinity for insulin of recombinant IgG1 Abs constructed by site-directed mutagenesis and consisting of partial germ-line revertants of mAb13. We found that the somatic point mutations in the mAb13 V_H, in particular the Arg at position 58, but not in the Vκ segment, were crucial in increasing the binding affinity for insulin. The increased affinity for insulin mediated by the mutated Arg58 residue contrasted with the complete loss of insulin-binding resulting from the substitution of Asn52 with Lys in the same V_H

[4]Abbreviations used in this paper: IDDM, insulin-dependent diabetes mellitus; Av_{rel}, relative avidity; CDR, complementarity-determining region; FR, framework region; K_d, dissociation equilibrium constant; K_{off}, dissociation (off) rate constant; K_{on}, association (on) rate constant; NP, 4-hydroxy-3-nitrophenyl-acetyl; phOx, 2-phenyl-5-oxazolone; PMN, polymorphonuclear cell; R, replacement (mutation); RF, rheumatoid factor; S, silent (mutation); H chain, heavy chain; L chain, light chain.

segment. Thus, human insulin has the potential to recruit and drive through affinity maturation natural autoantibody-producing cell clones expressing surface receptor for Ag in unmutated configuration.

Materials and Methods

Cloning and sequencing of the mAb13 V_H and Vκ genes

The anti-human insulin IgG1 κ mAb13 was generated by EBV-transformation and somatic cell hybridization of peripheral B cells from an IDDM patient treated with human recombinant insulin (12). The nucleotide and deduced amino acid sequences of the mAb13 V_HDJ_H and VκJκ genes have been reported (13), and are depicted in Figure 1, *A* and *B*, respectively. The germ-line V_H gene that gave rise to the expressed mAb13 V_H gene was cloned and sequenced from genomic DNA of autologous PMNs (13G12 sequence) (13). To isolate the putative germ-line gene that gave rise to the mAb13 Vκ segment, we performed PCR amplification of genomic DNA from autologous PMNs using the κ-Ov2 and κIII-FR3 B primers encompassing FR1 (residues 1–21) and FR3 sequences (residues 241–268) (Fig. 1*A* and Table I). The amplified products were cloned and sequenced using reported procedures (13).

Expression vectors

The features of the pcDNAIG and pSXRDIG plasmid vectors used for the in vitro expression of the human Ig V_HDJ_H and VκJκ gene segments, respectively, have been reported (18, 19). Briefly, pcDNAIG is a mammalian expression vector derived from pcDNAI/Neo (Invitrogen Corp., San Diego, CA), and encodes a whole human IgG1 H chain, preceded by a murine leader sequence. The H chain leader sequence (including the leader intron), the V_HDJ_H gene segment, and the Cγ1 gene are accommodated in a 2.3-kbp segment between *Hind*III and *Xba*I sites, and are driven by a human CMV promoter. The vector contains an RSV LTR-driven neomycin resistance gene. pSXRDIG is a mammalian expression vector derived from pUC18, and encodes a whole human Ig κ L chain, preceded by a murine leader sequence. The κ L chain leader sequence (including leader intron), the Ig VκJκ gene segment, and the human *C*κ gene are accommodated in a 1.3-kbp segment between *Hind*III and *Xba*I sites, and are driven by a SV40 promoter. The vector also contains the *DHFR* gene for selection by methotrexate.

Introduction of the mAb13 V_HDJ_H gene segment into pcDNAIG vector

The unique *Hind*III and *Xho*I sites, 5′ and 3′, respectively, of the leader-V_HDJ_H gene segment in the pcDNAIG vector were utilized for the introduction of the rearranged mAb13 V_HDJ_H gene segment, as reported (19). Briefly, the mouse H chain leader sequence of pcDNAIG and the V_HDJ_H gene segment of mAb13 were amplified in separate PCR (PCR 1 and PCR 2), and joined by recombinant PCR to yield the recombinant "leader-V_HDJ_H13" gene segment (Fig. 2*A*). Table I lists the sequences of the H leader and H-Ov1 primers used to amplify the vector leader sequence, and the H-Ov2 and H-FR4 primers used to amplify the mAb13 V_HDJ_H gene segment. The primers used at the ends to be joined (H-Ov1 and H-Ov2) were made complementary to one another by including a sequence complementary to the 3′ portion of the other primer. This made the products of PCR 1 and PCR 2 overlap at

the end to be joined, and allowed for the recombinant PCR by addition of excess H leader and H-FR4 primers (19). The recombinant fragment was sequenced to ensure that no unintended mutations were introduced during PCR amplification (4, 8, 13), digested with *Hind*III and *Xho*I, and then ligated into pcDNAIG previously digested with *Hind*III and *Xho*I and freed of its original V_HDJ_H gene segment. The recombinant pcDNAIG plasmid was amplified by transformation of competent MC1061/P3 cells (Invitrogen Corp.), and selection with ampicillin and tetracycline. The plasmid DNA was isolated using the Qiagen plasmid kit (Qiagen Inc., Chatsworth, CA).

Introduction of mAb13 VκJκ gene segment into pSXRDIG vector

The unique *Hind*III and *Xho*I sites, 5′ and 3′, respectively, of the leader-VκJκ gene segment in the pSXRDIG vector, were utilized for the insertion of the mAb13 VκJκ gene segment. The murine κ-leader sequence of pSXRDIG and the mAb13 VκJκ gene segment were amplified in separate PCR and joined by recombinant PCR (Fig. 2*A*). The sequences of the primers used for these PCR are listed in Table I. The recombinant leader-VκJκ13 gene segment was inserted into pSXRDIG after digestion with *Hind*III and *Xho*I. Recombinant pSXRDIG plasmids were amplified by transformation of competent DH5α cells and selection with ampicillin.

Construction of the "germ-line revertant" V_H13G12-DJ_H13 and Vκ13K20-Jκ13 gene segments

The method used to construct the leader-V_H13G12-DJ_H13 or leader-Vκ13K20-Jκ13 gene segment is schematized in Figure 2*B*. The FR1 through FR3 area of the autologous germ-line V_H 13G12 gene sequence was PCR amplified using the H-Ov2 and GIII-FR3 B primers (Fig. 1*A* and Table I). The FR3 through FR4 area of mAb13 V_HDJ_H gene segment was PCR-amplified using the GIII-FR3 A (the reverse complement of GIII-FR3 B) and H-FR4 primers (Table I). The two amplified fragments were purified and joined by recombinant PCR. The recombinant gene fragment was purified and then juxtaposed to the mouse H chain leader sequence by another recombinant PCR to yield the leader-V_H13G12-DJ_H13 gene segment sequence. Analogously, the FR1 through FR3 area of the autologous germ-line Vκ13K20 gene segment was PCR-amplified using the κ-Ov2 and κIII-FR3 B primers (Fig. 1*A* and Table I), and the FR3 through FR4 area of mAb13 VκJκ gene segment was PCR amplified using the κIII-FR3 A (reverse complement of κIII-FR3 B) and κ-FR4 primers (Table I). The two amplified fragments were purified and joined by recombinant PCR, and then juxtaposed to mouse κ leader sequence by another recombinant PCR to yield the leader-Vκ13K20-Jκ13 gene segment.

Construction of the partial germ-line revertants of the mAb13 V_HDJ_H gene segment

The method used to construct the partial germ-line revertant "Gly31" (identical to the V_H13G12-DJ_H13 except for the replacement of Ser31 by Gly) is schematized in Figure 2*C*. The leader through FR2 area of the leader-V_HDJ_H13 gene segment was PCR-amplified using the H leader and the FR2 B primers (Table I). The FR2 through FR4 area of the leader-V_H13G12-DJ_H13 gene segment was PCR amplified using the FR2-A and the H-FR4 primers (Table I). The two amplified fragments were purified and joined by recombinant

PCR. The same primers and recombinant PCR were used for the construction of the "Thr56, Arg58" (identical to the V_H13G12-DJ_H13 except for the replacement of Ser56 and Ser58 by Thr and Arg, respectively). The partial germ-line revertants "Thr56" and "Arg58" were constructed by recombinant PCr using the mutagenized primers listed in Table I and the leader-V_H13G12-DJ_H13 gene segment as a template. The variant of full germ-line revertant "Lys52" (identical to the V_H13G12-DJ_H13 except for the replacement of Asn52 by Lys) was generated by misincorporation of G instead of T at position 156 in one of the experiments aimed at the construction of the leader-V_H13G12-DJ_H13 gene segment.

Cell culture and transfection

Mammalian F3B6 cells were used for all transfection experiments. F3B6 is the Ig nonsecretor human-mouse heterohybridoma used as fusion partner for the generation of mAb13 (12, 19). F3B6 cells were cultured in RPMI 1640 (BioWhittaker, Walkersville, MD) with 10% FCS, 1% L-glutamine and antibiotics (FCS-RPMI), washed and then resuspended in FCS-RPMI at 10^7/ml. Cell suspension (750 μl) containing pcDNAIG (4 μg) and pSXRDIG (4 μg) vector DNA was transferred into an ice-cold electroporation cuvette with a 0.4 cm gap (Invitrogen Corp.). An electric pulse of 750 V/cm with a capacitance of 1000 μF was applied to the cell suspension using an Electroporator (Invitrogen Corp.) and a BRL Model 4000 power supply (Life Technologies, Inc., Gaithersburg, MD) (19). After electroporation, the cuvette was kept on ice for 10 min. Cells were then transferred to a flask containing 10 ml of pre-warmed FCS-RPMI. After a 48-h culture, the cell suspension was changed to selective medium containing 0.4 mg/ml of G418 (Geneticin, Life Technologies, Inc.), and cells were distributed into 96-well flat-bottom plates. Neomycin only was used as selecting agent, because in transfectants expressing only pcDNAIG (H chain), the accumulation of unsecretable H chain molecules leads to cell death. Clumps of transformant cells were detected within 7 to 10 days. After 2 wk, culture fluids were tested by ELISA using plates coated with goat $F(ab')_2$ fragment to human Ig $\mu + \gamma + \alpha$ H chains. Double γ1 and κ chain producer cells were identified by developing separate ELISA plates with peroxidase-conjugated affinity-purified goat anti-human Ig γ- and κ-chain (Cappel, Organon Teknika Corp., Durham, NC) (8, 12, 19, 20). In each transfection, 5 to 12 clones secreting IgG κ were generated. The three most efficient secretors were expanded and frozen.

Ab purification and ELISA

IgG mAb were purified from culture supernatant by 50% ammonium sulfate precipitation followed by absorption of solubilized IgG onto a GammaBind G-Sepharose column (Pharmacia LKB Biotechnology, Piscataway, NJ), and elution with 100 mM glycine-HCl buffer (pH 2.7). Eluates were brought to pH 7.5 by addition of neutralizing buffer (pH 9.0), dialyzed against PBS, and stored in aliquots at 4°C. mAb concentration and binding to human recombinant insulin (Eli Lilly Research Laboratories, Indianapolis, IN), ssDNA, human recombinant IL-1β (BASF Biotech Corp., Worcester, MA), tetanus toxoid, and *Escherichia coli* β-galactosidase were measured using appropriate ELISA, as previously described (12, 20, 21). Binding of the recombinant Abs to soluble insulin was analyzed by an ELISA-based competitive inhibition assay (4, 8, 12, 20, 21), and expressed as relative avidity (Av_{rel}). Av_{rel} represents concentration of soluble insulin, which inhibited by 50% the Ab binding to solid-phase insulin.

Measurement of IgG on-rate (K_{on}) and off-rate (K_{off}) for and from, respectively, immobilized insulin

Rate constants (K_{on} and K_{off}) of the interaction between recombinant IgG molecules and immobilized human insulin were measured using a real-time biospecific interaction analytical system (BIAcore system, Pharmacia Biosensor AB, Uppsala, Sweden) (22). Immobilization of human recombinant insulin to sensor chip CM5 was performed as follows: 1) a continuous flow (5 μl/min) of HBS (10 mM HEPES, 0.15 M NaCl, 3.4 mM EDTA, 0.05% surfactant P20) (pH 7.4) over the sensor surface was established and maintained; 2) the carboxylated dextran matrix was activated by injection of 20 μl of a solution containing 0.2 M *N*-ethyl-*N*′-3 diethyl-aminopropyl-carbodiimide (EDC) and 0.05 M *N*-hydroxysuccinimide (NHS); and 3) 20 μl of human recombinant insulin (100 μg/ml in 10 mM $C_2H_3NaO_2$ buffer pH 4.2) were injected followed by 20 μl of 1 M ethanolamine-hydrochloride pH 8.5 to block remaining NHS-ester groups, and achieved an immobilization level of 300 to 350 RU (resonance unit). Abs were analyzed in six different cycles of injection at six different concentrations (20 to 600 nM), to obtain sensograms that reflect the real-time Ab binding to immobilized insulin on the surface. Each analytical cycle was as follows: 1) purified Ab in HBS was injected and allowed to react with immobilized insulin for 20 min at a flow rate of 2 μl/min (Ab injection phase); 2) after injection, HBS was allowed to flow over the surface for 10 min (Ab dissociation phase); and 3) the surface was then regenerated by a 2-min injection of 100 mM NaOH. On-rate constant (K_{on}) was calculated based on the analysis of the Ab injection phase curve of the sensogram. In each analytical cycle, binding rates (dR/dt (RU/s)) were plotted vs relative responses (R (RU)). For example, binding rate at the time point of *n* (s) was calculated according to the equation dR/dt = (Rn+1 + Rn+2 + Rn+3 − Rn−1 − Rn−2 − Rn−3)/12, where Rn+1, Rn+2, Rn+3, Rn −1, Rn−2, and Rn−3 are the RU at the time point of n+1, n+2, n+3, n−1, n−2, and n−3, respectively. Based on the plotting, the slope value (K_s (1/s)) was obtained according to the equation dR/dt = constant − K_sR. Slope values (K_s (1/s)) from six cycles were plotted vs Ab (C (nM)), and the K_{on} was derived from the slope of this plotting curve according to the equation $K_s = K_{on}C + K_{off}$. Off-rate constant (K_{off}) was calculated based on the analysis of the Ab dissociation phase curve of the sensogram. In the analytical cycle involving the highest Ab concentration, log(R1/Rn) were plotted vs t*n*-t*1*, where R1 and t1 are the response level and time, respectively, at the beginning of dissociation, and R*n* and t*n* are those at the time point of *n*. The K_{off} was derived from the slope of the plotting curve, according to the equation log(R1/Rn) = K_{off} (t*n*-t*1*).

Results

Cloning of the mAb13 V_H and Vκ segment-related autologous germ-line genes

We have previously reported the isolation of the germ-line V_H gene sequence, designated as 13G12, that putatively gave rise to the somatically mutated mAb13 V_H gene (13). The 13G12 gene sequence is identical to that of the human germ-line H11 gene (23) except for GC instead of CG at residues 176–177. When compared with the sequence of the 13G12 gene, that of the mAb13 V_H segment displayed four somatic point-mutations, resulting in three amino acid replacements: Gly31 in CDR1, Thr56 and Arg58 in CDR2 (Fig. 1, *A* and *B*).

The mAb13 Vκ gene sequence displayed the highest degree of identity (97.9%, excluding the leader) to that of the germ-line *kv3g* gene, originally reported as Vg (24, 24a). Compared with this germ-line gene sequence, that of the mAb13 Vκ segment (residues 1 through 285) displayed a total of six putative point mutations, all resulting in amino acid replacements (Figs. 1, *A* and *B*). One replacement was in CDR1 and five in FR. To verify that *kv3g*, the germ-line gene that putatively gave rise to the expressed mAb13 VκIII segment, was actually present in the genome of the patient source of mAb13, we PCR amplified DNA from autologous PMNs using the k-Ov2 and the κIII-FR3 B primers, encompassing FR1 and FR3 sequences shared by the *kv3g* and mAb13 VκIII genes. Amplified DNA was cloned. The sequences of the 10 independent clones (13K04, 13K07, 13K09, 13K11, 13K12, 13K16, 13K17, 13K18, 13K20, 13K23) analyzed are depicted in Figure 3. Because eight clones yielded four discrete pairs of identical sequences (13K07 identical to 13K09; 13K11 identical to 13K12; 13K16 identical to 13K17; 13K20 identical to 13K23), a total of six different sequences were identified (13K04 and 13K18 were different and unique). Five sequences from eight clones (13K16 and 13K17; 13K18; 13K04; 13K07 and 13K09; 13K11 and 13K12) were 93.2 to 98.6% identical to that of *kv3g*, and 90.5 to 95.9% identical to that of the mAb13 Vκ gene segment (Fig. 3 and Table II). The 13K11/13K12 and 13K18 sequences were identical throughout the overlapping area to those of the germ-line *kv3g″* (24,24a) and *kv325* genes (24b), respectively. The sixth sequence, that of clones 13K20 and 13K23, was identical to the sequence of the germ-line *kv3g* gene throughout the 219 nucleotide overlapping area (Fig. 1*A* and Table II). We assumed the isolated 13K20/13K23 germ-line Vκ sequence to be identical to that of the *kv3g* gene throughout the FR1 and CDR3 areas, and we regarded it as that of the gene that gave rise to the mAb13 Vκ segment.

Insulin binding by the revertant mAb13 encoded by autologous germ-line genes

To investigate the possibility that insulin was the Ag originally responsible for the selection of the mAb13-producing cell clone, we set up to test the hypothesis that insulin could be specifically bound by the unmutated Ig gene product expressed by a B cell that was the putative progenitor of the mAb13-producing cell. To this end, we designed the full germ-line revertant of mAb13, utilizing the autologous germ-line 13G12 V_H and 13K20 Vκ genes, to be expressed in vitro as a human IgG1. First, to verify the effectiveness of our gene recombination and in vitro expression systems, we inserted the mutated V_HDJ_H and VκJκ gene segments of mAb13 into the pcDNAIG and pSXRDIG vectors, respectively, and expressed these gene segments by co-transfection of F3B6 cells. Nine stable transformant clones secreting human IgG1 κ were generated, three of which were expanded for Ab production. The recombinant IgG1 κ molecule, designated as V_HDJ_H13/VκJκ13, bound to insulin in a dose-saturable fashion and with an efficiency similar to that of the original somatic cell hybrid-produced mAb13 (13), but to none of the other Ags tested (Fig. 4*A*).

In order to generate the full germ-line revertant of mAb13, we constructed the V_H13G12-DJ_H13 gene segment by juxtaposing the autologous germ-line 13G12 gene sequence with the mAb13-derived DJ_H sequence, and the Vκ13K20-Jκ13 gene segment by juxtaposing the autologous germ-line 13K20 gene sequence with the mAb13-derived Jκ gene segment. The deduced amino acid sequences of these constructs are depicted in Figure 1*B*. The recombinant V_HDJ_H and VκJκ gene segments were inserted into pcDNAIG and pSXRDIG,

respectively, and expressed by co-transfection to F3B6 cells to yield the recombinant IgG1 molecule designated as V_H13G12-DJ_H13/Vκ13K20-Jκ13, and representing the full germ-line revertant of mAb13. Like the V_HDJ_H13/VκJκ13 IgG1, the V_H13G12-DJ_H13/Vκ13k20-jκ13 IgG1 bound to insulin in a dose-saturable fashion, but bound to none of the other Ags tested (Fig. 4*B*). To compare the insulin-binding activity of the germ-line revertant IgG1 to that of the wild-type somatically mutated mAb13, we performed competitive inhibition experiments using the recombinant V_H13G12-DJ_H13/Vκ13K20-Jκ13 IgG1 and V_HDJ_H13/VκJκ13 IgG1 molecules. The relative binding of these recombinant IgG1 to solid-phase insulin in the presence of different concentrations (2.5×10^{-10} to 2.5×10^{-7} g/μl) of soluble insulin are depicted in Figure 5. The Av_{rel} for insulin of the somatically mutated V_HDJ_H13/VκJκ13 IgG1 (Table III) was about three-fold higher than that of the unmutated V_H13G12-DJ_H13/Vκ13K20-Jκ13 IgG1 (1.69×10^{-8} g/μl). Thus, reversion to germ-line configuration of the somatically mutated mAb13 resulted in an Ab of lower binding affinity but still highly specific for insulin.

Relative contribution of the V_H and Vκ segments to the enhanced insulin binding by mAb13

To analyze the contribution of the mutated V_H and/or Vκ segments to the increased Av_{rel} of mAb13 for insulin, we constructed: 1) the recombinant V_H13G12-DJ_H13/VκJκ13 IgG1, consisting of the unmutated V_H segment paired with the mutated (mAb13) Vκ segment, and 2) the recombinant V_HDJ_H13/Vκ13K20-Jκ13 IgG1, consisting of the mutated V_H segment paired with the unmutated Vκ segment. The binding of these recombinant IgG1 molecules to soluble insulin was measured by competitive inhibition assays. The curve derived from the experiments involving the V_H13G12-DJ_H13/VκJκ13 IgG1 was similar to that derived from the analysis of the V_H13G12-DJ_H13/Vκ13K20-Jκ13 IgG1, whereas the competitive inhibition curve derived from the analysis of the V_HDJ_H13/Vκ13K20-Jκ13 IgG1 was similar to that derived from the analysis of the V_HDJ_H13/VκJκ13 IgG1 (Fig. 5). The Av_{rel} for insulin of the V_HDJ_H13/Vκ13K20-Jκ13 IgG1 (5.70×10^{-9} g/μl) was comparable to that of the V_HDJ_H13/VκJκ13 IgG1 (Table III), and was about threefold that of the V_H13G12-DJ_H13/VκJκ13 IgG1 (Table III) or that of the V_H13G12-DJ_H13/Vκ13K20-Jκ13 IgG1 (1.69×10^{-8} g/μl). These results suggest that the somatic mutations in the V_H segment, not those in the Vκ segment, predominantly contributed to the increased insulin affinity of mAb13 when compared to its full germ-line revertant counterpart.

To further analyze the contribution to insulin binding by the wild-type mutated and the germ-line revertant H chains, we performed kinetic analyses of the interaction between immobilized insulin and recombinant IgG1 molecules with different V_H mutational configurations. We calculated the insulin association rate constant (K_{on}), dissociation rate constant (K_{off}), and affinity (K_d) for the V_HDJ_H13/VκJκ13 IgG1 and V_H13G12-DJ_H13/VκJκ13 IgG1 utilizing the BIAcore system. The K_{off} from insulin of the V_HDJ_H13/VκJκ13 IgG1 was three- to fourfold lower than that of the V_H13G12-DJ_H13/VκJκ13 IgG1, whereas the K_{on} for insulin of these two recombinant Abs were virtually identical (Table III). Accordingly, the K_d value ($=K_{off}/K_{on}$) for insulin of the of the V_HDJ_H13/VκJκ13 IgG1 was about threefold lower (higher affinity) than that of the V_H13G12-DJ_H13/VκJκ13 IgG1 (Table III). These results show that the increased affinity

for insulin of the recombinant IgG1 containing the mutated mAb13 V_H segment reflects its decreased K_{off} from insulin.

Impact of individual replacement mutations in the mAb13 V_H segment on insulin binding

To determine whether the replacement mutation in the mAb13 V_H segment CDR1 or those in the CDR2 were responsible for the increased affinity of the mAb13 for insulin, we constructed the recombinant "Gly31" V_HDJ_H gene segment which was identical to V_H13G12-DJ_H13 except for the replacement of Ser31 by Gly, and the "Thr56, Arg58" V_HDJ_H gene segment, which is identical to V_H13G12-DJ_H13 except for the replacement of Ser56 and Ser58 by Thr and Arg, respectively. These recombinant V_HDJ_H gene segments were inserted into the pcDNAIG vectors, and were separately expressed by transfection of F3B6 cells in conjunction with the VκJκ13 gene segment to yield the "Gry31"/VκJκ13 IgG1 and "Thr56, Arg58"/VκJκ13 IgG1 molecules. As shown in Table III, the Av_{rel}, rate constants, and K_d of the "Gly31"/VκJκ13 IgG1 and "Thr56, Arg58"/VκJκ13 IgG1 were comparable to those of the V_H13G12-DJ_H13/VκJκ13 IgG1 and V_HDJ_H13/VκJκ13 IgG1, respectively, indicating that the mutations in the CDR2, i.e., Thr56 and Arg58, not those in the CDR1, played a crucial role in increasing the affinity of mAb13 for insulin.

To determine the relative contribution of the V_H segment CDR2 Thr56 and Arg58 amino acid replacements to the increased affinity for insulin, we constructed two additional recombinant V_HDJ_H gene segments, the "Thr56" which is identical to V_H13G12-DJ_H13 except for the replacement of Ser56 by Thr, and the "Arg58" which is identical to the V_H13G12-DJ_H13 except for the replacement of Ser58 by Arg. These recombinant V_HDJ_H gene segments were inserted into the pcDNAIG vectors and were separately expressed by transfection of F3B6 cells in conjunction with the VκJκ13 gene segment to yield the recombinant "Thr56"/VκJκ13 IgG1 and "Arg58"/VκJκ13 IgG1 molecules. As shown in Table III, the Av_{rel}, rate constants, and K_d of "Thr56"/VκJκ13 IgG1 and "Arg58"/VκJκ13 IgG1 (whose binding curve to insulin is depicted in Figure 4*C*) were comparable to those of the V_H13G12-DJ_H13/VκJκ13 IgG1 and V_HDJ_H13/VκJκ13 IgG1, respectively, indicating that the replacement of Ser58 by Arg, not that of Ser56 by Thr, was responsible for the increased affinity of mAb13 for insulin.

We further explored the role of a single amino acid replacement in insulin binding by the putative germ-line progenitor of mAb13. During the procedures aimed at constructing the full germ-line revertant mAb13, we generated, as a result of PCR misincorporation, the variant "Lys52" V_HDJ_H segment, which is identical in sequence to V_H13G12-DJ_H13 except for the replacement of Asn52 by Lys in CDR2. The "Lys52" V_HDJ_H segment was expressed in conjunction with the VκJκ13 gene to yield the "Lys52"/VκJκ13 IgG1 molecule. The single Lys52 amino acid replacement completely abrogated the binding of the V_H13G12-DJ_H13/VκJκ13 IgG1 molecule to insulin (Fig. 4*D*).

Discussion

In the present studies, we generated the full germ-line revertant of the somatically mutated antiinsulin IgG mAb13 using autologous germ-line V_H and Vκ gene sequences. Our experimental system therefore enabled us to recreate the unmutated Ig gene product of the

putative mAb13-producing cell clone B cell progenitor, although we had no clues whether somatic mutations, if any, were present in the mAb D gene segment. The recombinant germ-line revertant V_H13G12-DJ_H13/Vκ13K20-Jκ13 Ab bound specifically to insulin, suggesting that unmutated human Ig V genes can encode an insulin-specific binding site. In previous studies, we demonstrated that both polyreactive and monoreactive natural Abs binding foreign Ag and encoded by unmutated or minimally mutated genes can be isolated from the normal human B cell repertoire (6, 11, 25, 26). The anti-self Ag reactivity of most natural Abs in germ-line configuration so far reported has been thought to be a function of their polyreactivity (5, 6, 11, 25–29). The expressed insulin-specific V_H13G12-DJ_H13/Vκ13K20-Jκ13 constructs, reported here, possibly represent the first direct evidence of a monoreactive self Ag-binding site encoded by unmutated human V_H and V_L genes, and offer a structural basis for our previous demonstration of naturally occurring monoreactive autoantibodies to insulin in the normal B cell repertoire (12).

In a B cell, the unmutated Ig receptor for Ag needs to display binding specificity for the selecting ligand to allow for clonotype recruitment toward affinity maturation (14, 15, 30–32). The ability of the full germ-line revertant of mAb13 to bind insulin specifically, as demonstrated here, provides indirect evidence that insulin was the Ag responsible for the in vivo activation, amplification, and selection of the specific anti-insulin mAb13-producing cell clone. Once Ab producing cell progenitors enter the Ag-dependent phase of B cell differentiation, they come under strong selective pressure. Somatic point-mutations arise and accumulate in the Ig V genes, and give rise to relatively large numbers of clones with a nonpermissive structure or reduced affinity for Ag (32, 33). Based on the number of invariant and conserved residues compiled by Kabat et al. (34), Shlomchik et al. (35) estimated that half the mutations in FR would be deleterious to the preservation of a sound Ab structure. Based on the structural analysis of the Abs derived from immune responses to influenza virus hemagglutinin (36) and 4-hydroxy-3-nitrophenylacetyl (NP) (37), it was estimated that 25 to 50% of randomly acquired mutations would be detrimental to Ag binding. Experiments by Chen et al. (38) of random mutagenesis of the V_H segment CDR2 of murine anti-posphocholine (PC) T15 Abs revealed that 43% of randomly mutated, unselected Abs lost their Ag-binding ability. The present demonstration that only one amino acid replacement in the V_H segment CDR2 (Asn→Lys at position 52) totally abolishes the ability of the putative germ-line mAb13 precursor to bind insulin further emphasizes the Ab susceptibility to binding loss resulting from somatic mutations.

The present study is, to the best of our knowledge, the first direct delineation of intraclonal affinity maturation of a human autoantibody response through somatic mutation and Ag-driven selection. Although the difference in affinity between the unmutated and somatically-mutated mAb13 was relatively small (about three-fold), it might have led to substantial changes in receptor cross-linking, Ag processing, and presentation, which are crucial early stages in the process of B cell recruitment, Ab production, and affinity maturation. Site-directed mutagenesis experiments by Sharon (39) have demonstrated that a 200-fold increase in affinity of a murine anti-*p*-azophenylarsonate Ab can be achieved in a stepwise manner by three amino acid replacements in the V_H segment. A 10-fold increase in affinity resulting from only one amino acid replacement has been observed in murine anti-NP and

anti-2-phenyl-5-oxazolone (phOx) Abs (32, 40). These drastic changes in affinity as a result of single or few amino acid substitutions are likely a feature of hapten binding, which is mediated by a very small number (one to about four) of amino acid residues (41). Crystallographic analysis of different Ag-Ab complexes involving peptides or proteins has revealed that the Ag/Ab interface includes multiple contact CDR residues (up to about 20) accommodated in a relatively large surface (42–45). Accordingly, the impact of individual amino acid replacements on the binding affinity should be much smaller. Thus, the small difference in affinity between the unmutated and the wild-type mAb13 for insulin would reflect the light load of somatic mutations in relation to the relatively large Ag size (insulin molecular mass approximately 6,000 Da).

Consistent with the traces of Ag selection displayed by the mAb13 V_H segment (13), the present studies demonstrated that somatic mutations in the V_H segment, but not the Vκ segment, of mAb13 contributed to the increased affinity of mAb13 for insulin. The finding that the V_H segment was the primary target of insulin-driven selection is consistent with the notion that the H chain plays in many cases a primary role in determining the Ag specificity of Abs and autoantibodies (46–48). Although in some cases the L chain seems to play a critical role in defining epitope specificity (31, 49, 50), individual Ig H chains can bind Ag independently of the contribution of any L chain, as originally shown by Utsumi and Karush (51) in an isolated rabbit H chain to *p*-azophenyl-β-lactoside, and by Jaton et al. (52) in an isolated rabbit H chain to the 2,4-dinitrophenyl group. These early findings have been extended by recent experiments showing efficient Ag binding by cloned murine V_H domains, “single domain Abs”, to lysozyme or keyhole-limpet hemocyanin (53), and by the observation that a broad Ag-binding repertoire is provided by naturally occurring Ig H chain dimers in the camel (54). Finally, x-ray crystallography has demonstrated in at least three Ag-Ab systems that the number of H chain residues contacting Ag far exceeds that of the Ag-contacting residues in the L chain (41, 42, 45).

Analysis of the partial V_H germline revertants of mAb13 revealed that the Ser→Arg replacement at position 58 in the V_H segment CDR2 is responsible for the increased affinity of mAb13 for insulin. According to the conformational modeling of human Ig V_H segments by Chothia et al. (55), residue 58 would be located at the bottom portion of CDR2 loop of the V_H segment, and faces the cleft between the V_L CDR3 and the V_H CDR2 loops. Although the insulin specificity seems to be an inherent property of the mAb13 V_H segment (13), we have shown that replacement of the V_L CDR3 of mAb13 by that of some unrelated Ab results in the complete loss of insulin-binding activity (13, 19), suggesting that the region around the cleft between the VκCDR3 and the V_H CDR2 is involved in the insulin binding by mAb13. Thus, an amino acid replacement, particularly a nonconserved replacement, at residue 58 of mAb13 V_H segment can potentially affect the interaction between the mAb13 and insulin. Although we cannot formally exclude the possibility that the Ser→Arg replacement at position 58 resulted in an altered conformation of V_H segment CDR2, we prefer an alternative possibility, i.e., that amino acid replacement by positively charged Arg increased the electrostatic potential of the combining site, and consequently increased the attractive force for the negatively charged insulin molecule (13). Basic amino acids, particularly Arg, are known to bind insulin, and this interaction is the rationale for the

clinical use of protamine to delay insulin absorption. The H chain CDR3 of mAb13 displayed two single Arg and that of the mAb48, another human anti-insulin IgG, displayed an Arg triplet (13). The H chain CDR3s of two human anti-insulin IgM mAbs and in those of two mouse anti-insulin IgG mAb also display a number of Arg residues (56, 57). Arg residues are also characteristic of anti-DNA autoantibodies and are thought to play a major role in DNA binding (58, 59). In vitro mutagenesis experiments by Radic et al. (59) demonstrated that increased DNA binding affinity goes hand in hand with increased positive electrostatic potentials in the region of H chain CDR3 and along the V_H and V_L segment interface, suggesting that in anti-DNA autoantibodies, the major molecular mechanism of the increased affinity resulting from somatic point mutation could be the change in electrostatic potential.

Kinetic analysis of the recombinant IgG1 consisting of the wild-type Vκ chain and variably mutated V_H chains has revealed that affinity increase by Ser→Arg replacement at position 58 was attributed to the decrease in the off-rate (K_{off}). This phenomenon is reminiscent of the observations by Foot and Milstein (60) showing that in the murine response to phOx the intraclonal affinity maturation brought about by somatic mutations entails mainly a decrease in Ab off-rate (K_{off}), and virtually no change in on-rate (K_{on}). The authors suggested that there is a structural constraint on the on-rate (K_{on}), detectable as an “energy barrier”, which may be an intrinsic property of the conformation of the phOx-binding site, and that the inability to escape this constraint through point-mutation leads to the recruitment of new and kinetically superior (higher K_{on}) V_H/V_L clonotypes (60). Similar constraints may also influence the human Ab response to insulin. Whether such putative constraints in the human anti-insulin response are eventually overcome by recruitment of different and kinetically superior V_H/V_L clonotypes remains to be determined. The recruitment of these different clonotypes may be a crucial factor in the events leading to resistance and/or higher forms of resistance to insulin therapy in IDDM patients.

Acknowledgments

We are indebted to Dr. Kirk Fry (Genelabs Technologies, Inc., Redwood City, CA) for his generous gift of the pcDNAIG and pSXRDIG expression vectors, and the Eli Lilly Corp., Indianapolis, IN, for the gift of human recombinant insulin. We are grateful to Dr. Roberto J. Poljak for useful discussions. We thank Dr. Hideyuki Ikematsu for valuable suggestions and Nancy Pacheco for skillful technical assistance.

References

1. Van Es JH, Meyling FHJG, van de Akker WRM, Aanstoot H, Derksen RHWM, Logtenberg T. Somatic mutations in the variable regions of a human IgG anti-doublestrand DNA autoantibody suggest a role for antigen in the induction of systemic lupus erythematosus. J Exp Med. 1991; 173:461. [PubMed: 1899104]
2. Manheimer-Lory A, Katz JB, Pillinger M, Ghossein C, Smith A, Diamond B. Molecular characteristics of antibodies bearing an anti-DNA-associated idiotype. J Exp Med. 1991; 174:1639. [PubMed: 1660528]
3. Van Es JH, Aanstoot H, Gmelig-Meyling FHJ, Derksen RHWM, Logtenberg T. A human systemic lupus erythematosus-related anti-cardiolipin/single-stranded DNA autoantibody is encoded by a somatically mutated variant of the developmentally restricted 51p1 gene. J Immunol. 1992; 149:2234. [PubMed: 1517580]

4. Kasaian MT, Ikematsu H, Balow JE, Casali P. Structure of the V_H and V_L segments of monoreactive and polyreactive IgA autoantibodies to DNA in patients with SLE. J Immunol. 1994; 152:3137. [PubMed: 8144908]
5. Pascual V, Randen I, Thompson K, Sioud M, Forre O, Natvig JG, Capra JD. The complete nucleotide sequences of the heavy chain variable regions of six monospecific rheumatoid factors derived from Epstein-Barr virus-transformed B cells isolated from the synovial tissue of patients with rheumatoid arthritis. J Clin Invest. 1990; 86:1320. [PubMed: 2170450]
6. Harindranath N I, Goldfarb S, Ikematsu H, Burastero SE, Wilder RL, Notkins AL, Casali P. Complete sequence of the genes encoding the V_H and V_L regions of low- and high-affinity monoclonal IgM and IgA1 rheumatoid factors produced by $CD5^+$ B cells from a rheumatoid arthritis patient. Int Immunol. 1991; 3:865. [PubMed: 1718404]
7. Olee T, Lu EW, Huang DF, Soto-Gil RW, Deftos M, Kozin F, Carson DA, Chen PP. Genetic analysis of self-associating immunoglobulin G rheumatoid factors from two rheumatoid synovia implicates an antigen-driven response. J Exp Med. 1992; 175:831. [PubMed: 1740665]
8. Mantovani L, Wilder RL, Casali P. Human rheumatoid B-1a ($CD5^+$ B) cells make somatically hypermutated high affinity IgM rheumatoid factors. J Immunol. 1993; 151:473. [PubMed: 7686945]
9. Cunningham, M. Bacterial antigen mimicry. In: Bona, CA.; Siminovitch, K.; Zanetti, M.; Teofilopoulos, AN., editors. The Molecular Pathology of Autoimmune Diseases. Harwood Academic Publishers GmbH; Chur, Switzerland: 1993. p. 245-256.
10. Riboldi, P.; Kasaian, MT.; Mantovanni, L.; Ikematsu, H.; Casali, P. Natural antibodies. In: Bona, CA.; Siminovitch, K.; Zanetti, M.; Teofilopoulos, AN., editors. The Molecular Pathology of Autoimmune Diseases. Harwood Academic Pulishers GmbH; Chur, Switzerland: 1993. p. 45-64.
11. Harindranath N, Ikematsu H, Notkins AL, Casali P. Structure of the V_H and V_L regions of polyreactive and monoreactive human natural antibodies to HIV-1 and *E. coli* β-galactosidase. Int Immunol. 1993; 5:1523. [PubMed: 8312222]
12. Casali P, Nakamura M, Ginsberg-Fellner F, Notkins AL. Frequency of B cells committed to the production of antibodies to insulin in newly diagnosed patients with insulin-dependent diabetes mellitus and generation of high affinity monoclonal IgG to insulin. J Immunol. 1990; 144:3741. [PubMed: 2159034]
13. Ikematsu H, Ichiyoshi Y, Schettino EW, Nakamura M, Casali P. V_H and Vκ segment structure of anti-insulin IgG autoantibodies in patients with insulin-dependent diabetes mellitus: evidence for somatic selection. J Immunol. 1994; 152:1430. [PubMed: 8301143]
14. Griffiths GM, Berek C, Kaartinen M, Milstein C. Somatic mutation and the maturation of immune response to 2-phenyl-5-oxazolone. Nature. 1984; 312:271. [PubMed: 6504141]
15. McKean D, Huppi K, Bell M, Staudt L, Gerhard W, Weigert MG. Generation of antibody diversity in the immune response of BALB/c mice to influenza virus hemagglutinin. Proc Natl Acad Sci USA. 1984; 81:3180. [PubMed: 6203114]
16. Kocks C, Rajewsky K. Stable expression and somatic hypermutation of antibody V regions in B-cell developmental pathways. Annu Rev Immunol. 1989; 7:537. [PubMed: 2653375]
17. Chang B, Casali P. A major proportion of human Ig V_H genes displays CDR1 sequences inherently susceptible to amino acid replacement. Immunol Today. 1994; 15:367. [PubMed: 7916950]
18. Larrick JW, Wallace EF, Coloma MJ, Bruderer U, Lang AB, Fry K. Therapeutic human antibodies derived from PCR amplification of B-cell variable regions. Immunol Rev. 1992; 130:69. [PubMed: 1286873]
19. Ichiyoshi Y, Casali P. Analysis of the structural correlates for Ig polyreactivity by multiple reassortments of chimeric human immunoglobulin heavy and light chain V segments. J Exp Med. 1994; 180:885. [PubMed: 8064239]
20. Nakamura M, Burastero SE, Ueki Y, Larrick JW, Notkins AL, Casali P. Probing the normal and autoimmune B cell repertoire with Epstein-Barr Virus: frequency of B cells producing monoreactive high affinity autoantibodies in patients with Hashimoto's disease and systemic lupus erythematosus. J Immunol. 1988; 141:4165. [PubMed: 2848890]
21. Ueki Y I, Goldfarb S, Harindranath N, Gore M, Koprowski H, Notkins AL, Casali P. Clonal analysis of a human antibody response: quantitation of precursors of antibody-producing cells and

generation and characterization of monoclonal IgM, IgG, and IgA to rabies virus. J Exp Med. 1990; 171:19. [PubMed: 2153188]

22. Karlson R, Michaelsson A, Mattsson L. Kinetic analysis of monoclonal antibody-antigen interactions with a new biosensor based analytical system. J Immunol Methods. 1991; 145:229. [PubMed: 1765656]
23. Rechavi G, Bienz B, Ram D, Ben-Neriah Y, Cohen JB, Zakut R, Givol D. Organization and evolotion of immunoglobulin V_H gene subgroups. Proc Natl Acad Sci USA. 1982; 79:4405. [PubMed: 6812048]
24. Pech M, Zachau HG. Immunoglobulin genes in different subgroups are interdigitated within the Vκ locus. Nucleic Acids Res. 1984; 12:9229. [PubMed: 6440122]
24. Chen PP, Albrandt K, Kipp TJ, Radoux V, Liu F, Carson DA. Isolation and characterization of human VκIII germ-line genes. Implication for the molecular basis of human VκIII light chain diversity. J Immunol. 1987; 139:1727. [PubMed: 3114376]
24. Kipps TJ, Fong S, Tomhave E, Chen PP, Goldfien RD, Carson DA. High frequency expression of conserved kappa variable region gene in chronic lymphocytic leukemia. Proc Natl Acad Sci USA. 1987; 84:2916. [PubMed: 3106980]
25. Sanz I, Casali P, Thomas JW, Notkins AL, Capra JD. Nucleotide sequence of eight human natural autoantibodies V_H region reveals apparent restricted use of V_H families. J Immunol. 1989; 142:4054. [PubMed: 2497188]
26. Ikematsu H, Kasaian MT, Schettino EW, Casali P. Structural analysis of the $V_H(D)J_H$ segments of human polyreactive IgG mAb. Evidence for somatic selection. J Immunol. 1993; 151:3604. [PubMed: 8376796]
27. Chen PP, Liu MF, Sinha S, Carson DA. A 16/6 idiotype-positive anti-DNA antibody is encoded by a conserved V_H gene with no somatic mutation. Arthritis Rheum. 1988; 31:1429. [PubMed: 3263866]
28. Baccala R, Quang TV, Gilbert M, Ternynck T, Avrameas S. Two murine natural polyreactive autoantibodies are encoded by nonmutated germ-line genes. Proc Natl Acad Sci USA. 1989; 86:4624. [PubMed: 2499887]
29. Siminovitch KA, Mesiner V, Kwong PC, Song Q-L, Chen PP. A natural autoantibody is encoded by germline heavy and lambda light chain variable region genes without somatic mutation. J Clin Invest. 1989; 84:1675. [PubMed: 2509520]
30. Manser T, Gefter ML. The molecular evolution of the immune response: idiotype-specific suppression indicates that B cells express germ-line-encoded V genes prior to antigenic stimulation. Eur J Immunol. 1986; 16:1439. [PubMed: 3490986]
31. Kocks C, Rajewsky K. Stepwise intraclonal maturation of antibody affinity through somatic hypermutation. Proc Natl Acad Sci USA. 1988; 85:8206. [PubMed: 3263647]
32. Berek C, Milstein C. Mutation drift and repertoire shift in the maturation of the immune response. Immunol Rev. 1987; 96:23. [PubMed: 3298007]
33. Manser T, Parhami-Seren B, Margolies MN, Gefter ML. Somatic mutated forms of a major anti-*p*-azophenylarsonate antibody variable region with drastically reduced affinity for *p*-azophenylarsonate: by-products of an antigen-driven immune response? J Exp Med. 1987; 166:1456. [PubMed: 3681190]
34. Kabat, EA.; Wu, TT.; Perry, HM.; Gottesman, KS.; Foeller, C. Sequences of Proteins of Immunological Interest. 5. U. S. Department of Health and Human Services; Washington, DC: 1991.
35. Shlomchik MJ, Aucoin AH, Pisetsky DS, Weigert MG. Structure and function of anti-DNA autoantibodies derived from a single autoimmune mouse. Proc Natl Acad Sci USA. 1987; 84:9150. [PubMed: 3480535]
36. Caton AJ, Brownlee GG, Staudt LM, Gerhard W. Structural and functional implication of a restricted antibody response to a defined antigenic region on the influenza virus hemaglutinin. EMBO J. 1986; 5:1577. [PubMed: 2427335]
37. Cumano A, Rajewsky K. Clonal recruitment and somatic mutation in the generation of immunological memory to the hapten NP. EMBO J. 1986; 5:2459. [PubMed: 2430792]

38. Chen C V, Robert A, Rittenberg MB. Generation and analysis of random point mutations in an antibody CDR2 sequence: many mutated antibodies lose their ability to bind antigen. J Exp Med. 1992; 176:855. [PubMed: 1512548]
39. Sharon J. Structural correlates of high antibody affinity: three engineered amino acid substitutions can increase the affinity of an anti-*p*-azophenylarsonate antibody 200-fold. Proc Natl Acad Sci USA. 1990; 87:4814. [PubMed: 2352950]
40. Allen D, Simon T, Sablitzky F, Rajewsky K, Cumano A. Antibody engineering for the analysis of affinity maturation of an anti-hapten response. EMBO J. 1988; 7:1995. [PubMed: 3138111]
41. Segal DM, Padlan EA, Cohen GN, Radikoff S, Potter M, Davies DR. The three-dimensional structure of a phosphorylcholine-binding mouse immunoglobulin Fab and the nature of the antigen binding site. Proc Natl Acad Sci USA. 1974; 71:4298. [PubMed: 4530984]
42. Amit AG, Mariuzza RA, Phillips SEV, Poljak RJ. Three-dimensional structure of an antigen-antibody complex at 2.8 Å resolution. Science. 1986; 233:747. [PubMed: 2426778]
43. Sheriff S, Silverton EW, Padlan EA, Cohen GH, Smith-Gill SJ, Finzel BC, Davies DR. Three-dimensional structure of an antibody-antigen complex. Proc Natl Acad Sci USA. 1987; 84:8075. [PubMed: 2446316]
44. Padlan EA, Silverton EW, Sheriff S, Cohen GH, Smith-Gill SJ, Davies DR. Structure of an antibody-antigen complex: crystal structure of the HyHEL-10 Fab-lysozyme complex. Proc Natl Acad Sci USA. 1989; 86:5938. [PubMed: 2762305]
45. Stanfield RL, Fieser TM, Lerner RA, Wilson IA. Crystal structure of an antibody to a peptide and its complex with peptide antigen at 2.8 Å. Science. 1990; 248:712. [PubMed: 2333521]
46. Newkirk MM, Gram H, Heinrich GF, Oestberg L, Capra JD, Wasserman RL. Complete protein sequences of the variable regions of the cloned heavy and light chains of a human anti-cytomegalovirus antibody reveal a striking similarity to human monoclonal rheumatoid factors of the Wa idiotypic family. J Clin Invest. 1988; 81:1511. [PubMed: 2452836]
47. Radic MZ, Mascelli MA, Erikson J, Shan H, Weigert MG. Ig H and L chain contributions to autoimmune specificities. J Immunol. 1991; 146:176. [PubMed: 1898596]
48. Kabat EA, Wu TE. Identical V region amino acid sequences and segments of sequences in antibodies of different specificities: relative contributions of V_H and V_L genes, minigenes, and complementarity-determining regions to binding of antibody-combining sites. J Immunol. 1991; 147:1709. [PubMed: 1908882]
49. Sanz I, Capra JD. Vκ and Jκ gene segments of A/J Ars-A antibodies: somatic recombination generates the essential arginine at the junction of the variable and joining regions. Proc Natl Acad Sci USA. 1987; 84:1085. [PubMed: 3103124]
50. Portolano S, Chazenbalk GD, Hutchison JS, Mclachlan SM, Rapoport B. Lack of promiscuity in autoantigen-specific H and L chain combinations as revealed by human H and L chain “roulette”. J Immunol. 1993; 150:880. [PubMed: 8423344]
51. Utsumi S, Karush F. The subunits of purified rabbit antibody. Biochemistry. 1964; 3:1329. [PubMed: 14229677]
52. Jaton JC, Klinman NR, Givol D, Sela M. Recovery of antibody activity upon reoxidation of completely reduced polyalanyl heavy chain and its Fd fragment derived from anti-2,4-dinitrophenyl antibody. Biochemistry. 1968; 7:4185. [PubMed: 4973471]
53. Ward ES, Gussow D, Griffiths AD, Jones PT, Winter G. Binding activities of a repertoire of single immunoglobulin variable domains secreted from. Escherichia coli Nature. 1989; 341:544.
54. Hamers-Casterman C, Atarhouch T, Muyldermans S, Robinson G, Hamers C, Bajyana Songa E, Bendahman N, Hamers R. Naturally occurring antibodies devoid of light chains. Nature. 1993; 363:446. [PubMed: 8502296]
55. Chothia C, Lesk AM, Gherardi E, Tomlinson IM, Walter G, Marks JD, Llewelyn MB, Winter G. Structural repertoire of the human V_H segments. J Mol Biol. 1992; 227:799. [PubMed: 1404389]
56. Thomas JW. V region diversity in human anti-insulin antibodies: preferential use of a V_HIII gene subset. J Immunol. 1993; 150:1375. [PubMed: 8432983]
57. Ewulonu UK, Nell LJ, Thomas JW. V_H and V_L gene usage by murine IgG antibodies that bind autologous insulin. J Immunol. 1990; 144:3091. [PubMed: 2109009]

58. Shlomchik M, Mascelli M, Shan H, Radic MZ, Pisetsky D, Marshak-Rothstein A, Weigert MG. Anti-DNA antibodies from autoimmune mice arise by clonal expansion and somatic mutation. J Exp Med. 1990; 171:265. [PubMed: 2104919]

59. Radic MZ, Mackle J, Erikson J, Mol C, Anderson WF, Weigert M. Residues that mediate DNA binding of autoimmune antibodies. J Immunol. 1993; 150:4966. [PubMed: 8496598]

60. Foote J, Milstein C. Kinetic maturation of an immune response. Nature. 1991; 352:530. [PubMed: 1907716]

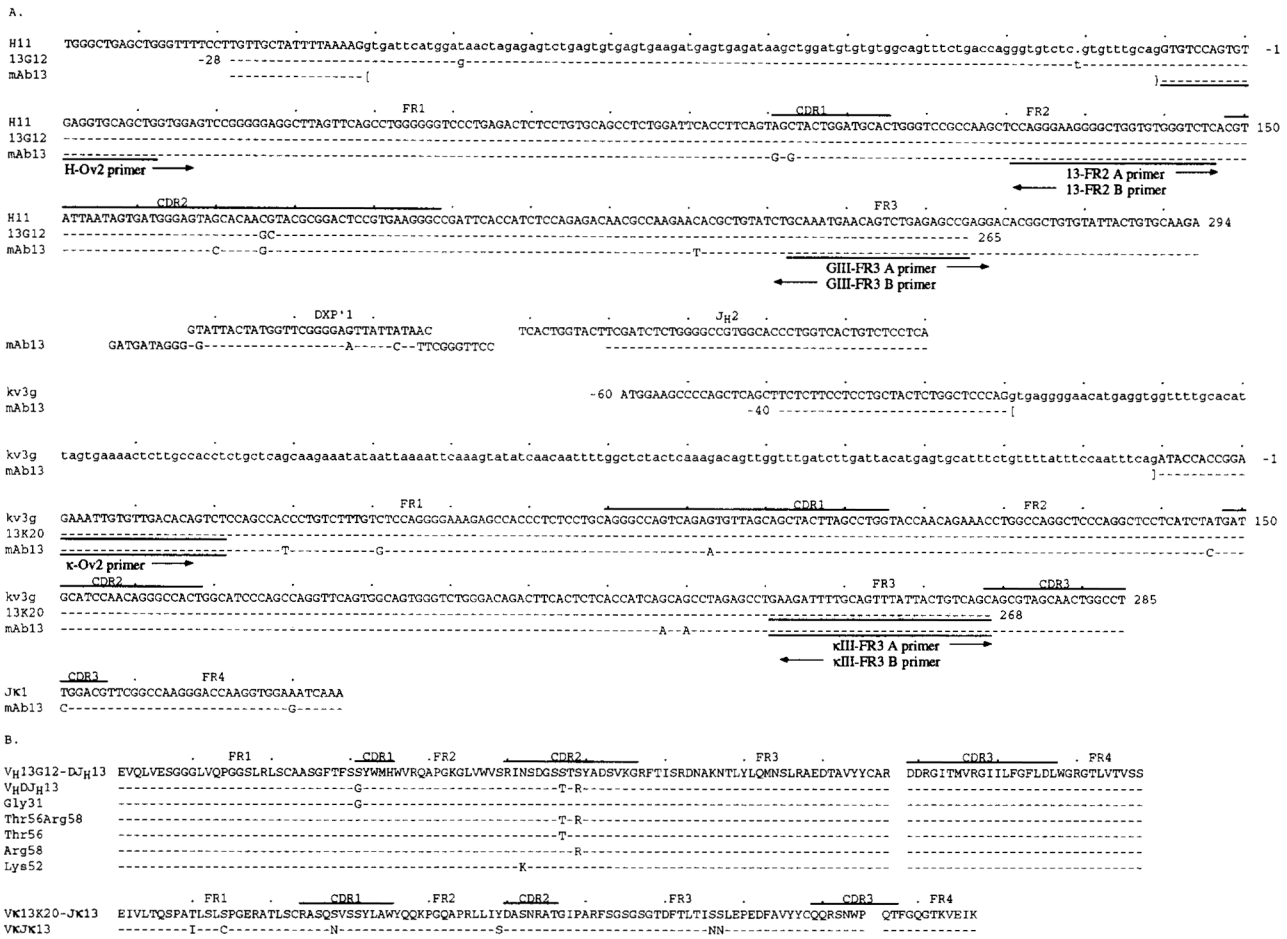

FIGURE 1.

Nucleotide sequences of the wild-type and germ-line mAb13 V_H, D-J_H, Vκ and Jκ gene segments (*A*); and deduced amino acid sequences of the wild-type and recombinant mAb13 V_HDJ_H and VκJκ gene segments (*B*). The top sequence in each cluster is that of the germ-line gene sequence to which the remaining sequences of the cluster are compared. 13G12 and 13K20 are the autologous germ-line sequences. Dashes indicate identities. Solid lines on top of each cluster depict CDR. Small letters denote untranslated sequences. The sequences or reverse complementary sequences encompassed by the H-Ov2, 13-FR2, GIII-FR3, κ-Ov2, and κIII-FR3 primers are underlined. The 13G12, mAb13 V_H segment, and mAb13 Vκ segment gene sequences are available from EMBL/GenBank under accession numbers D-16832, D-16833, and D-16834, respectively. For the EMBL/GenBank accession number of the germ-line 13K20 gene sequence see legend to Figure 3.

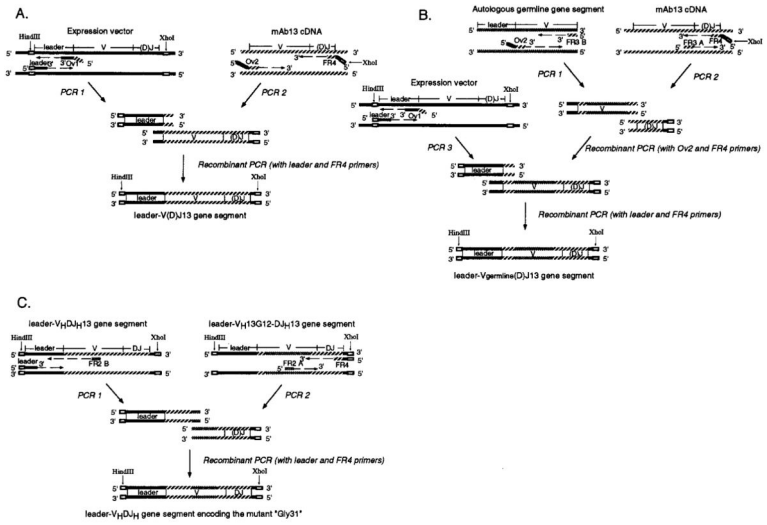

FIGURE 2.

Construction of the recombinant leader-V(D)J13 gene segment (leader-V_HDJ_H13 or leader-$V\kappa J\kappa 13$) (*A*), of the recombinant "leader-$V_{germ\text{-}line}$(D)J13" gene segment (*B*), and of the recombinant gene segment encoding the mutant "Gly31" (*C*). Open boxes depict restriction sites. Broken arrows indicate nucleotide chain elongation by DNA polymerase. Solid (▬), hatched (▨), and shaded (▩) segments depict the sequences of the expression vectors (pcDNAIG or pSXRDIG), that of the V(D)J gene segment of mAb13, and those of autologous germ-line genes, respectively. To construct the recombinant leader-V(D)J13 gene segment (leader-V_HDJ_H13 or leader-$V\kappa J\kappa 13$), the mouse leader Ig V gene segment in the expression vector and the V_HDJ_H or $V\kappa J\kappa$ gene segment of mAb13 were amplified in separate PCR (PCR 1 and PCR 2), and joined by recombinant PCR. Primers (Ov1 and Ov2) used at the end to be joined were made complementary to one another by including nucleotides at the 5′ end that are complementary to the 3′ portion of the other primer (see Table I). Primers, leader, and FR4 were designed to yield final recombinant products bearing *Hind*III and *Xho*I sites used for the introduction into the expression vectors. To construct the recombinant leader-$V_{germ\text{-}line}$(D)J13 gene segment, the gene segment amplified from the autologous germ-line gene using the sense Ov2 and antisense FR3 B primers (GIII-FR3 B or κIII-FR3 B) (PCR 1) and that amplified from the mAb13 V(D)J gene using the sense FR3 A (GIII-FR3 A or κIII-FR3 A) and antisense FR4 (PCR 2) were joined by recombinant PCR. This recombinant gene segment was fused to the mouse Ig leader sequence (amplified by PCR 3) by recombinant PCR. To construct the recombinant gene segment encoding the mutant "Gly31", the DNA segment amplified from the leader-V_HDJ_H segment using the leader and 13-FR2 B primers (PCR 1) and that amplified from the recombinant leader-$V_H13G12\text{-}DJ_H13$ segment using the 13-FR2 A and FR4 primers (PCR 2) were joined and amplified by recombinant PCR. See Table I for sequences of the sense 13-FR2 A and the antisense 13-FR2 B primers.

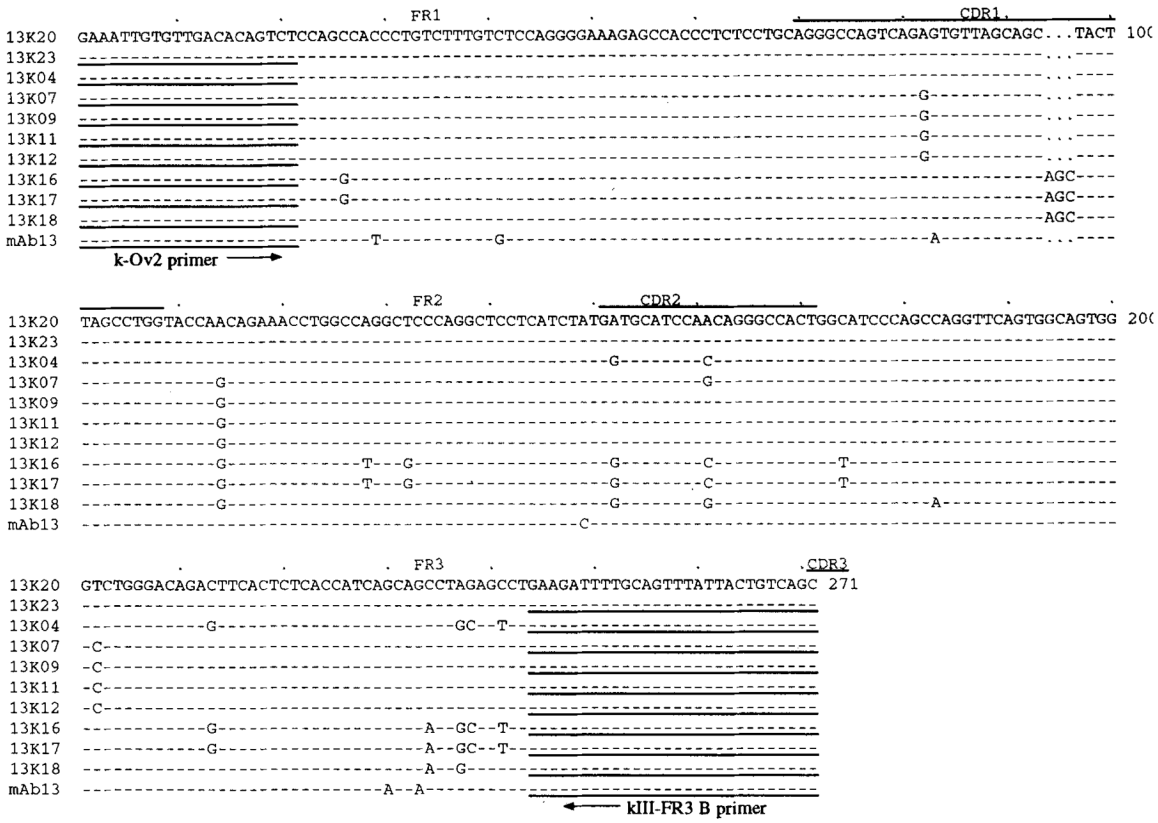

FIGURE 3.

Nucleotide sequences of the germ-line 13K20, 13K23, 13K04, 13K07, 13K09, 13K11, 13K12, 13K16, 13K17, and 13K18 Vκ gene segments isolated from PMN of the patients whose B cells were utilized for the generation of the mAb13-producing cell line. The top sequence (13K20, identical to that of the germ-line *kv3g* gene) is that to which the remaining sequences are compared. Dashes indicate identities. Solid lines on top of each cluster depict CDR. The sequences and reverse complementary sequences encompassed by the H-Ov2 and κIII-FR3 primers, respectively, are underlined. The germ-line 13K20/13K23, 13K04, 13K07/13K09, 13K11/13K12, 13K16/13K17, and 13K18 Vκ gene sequences are available from EMBL/GenBank under accession numbers L-37726, L-37728, L-37727, L-37725, L-37730, and L-37729, respectively.

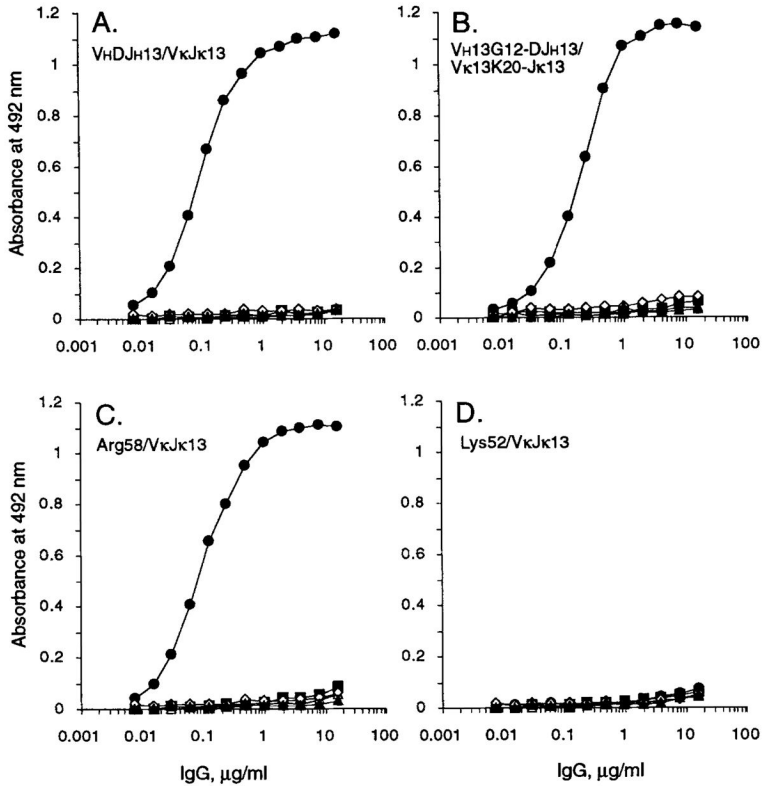

FIGURE 4.

Binding of the recombinant $V_HDJ_H13/V\kappa J\kappa 13$ (*A*), $V_H13G12\text{-}DJ_H13/V\kappa 13K20\text{-}J\kappa 13$ (*B*), Lys52/$V\kappa J\kappa 13$ (*C*), and Arg58/$V\kappa J\kappa 13$ (*D*) IgG1 Abs to human recombinant insulin (●), ssDNA (△), tetanus toxoid (■), human recombinant IL-1β (▲), *E. coli* β-galactosidase (◇), and BSA (□). The Ag-binding activity of each Ab to solid-phase Ag is expressed as optical absorbance at 492 nm.

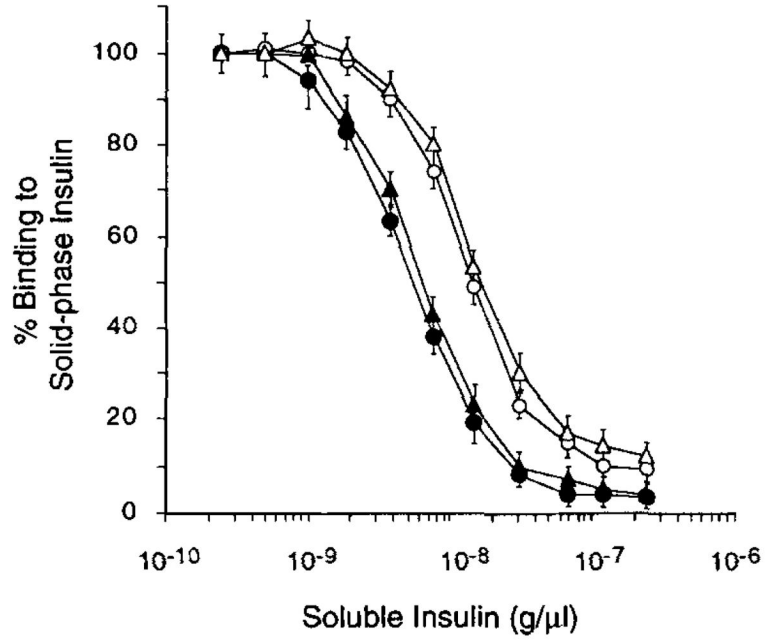

FIGURE 5.

Inhibition of the binding of the recombinant V_H-$DJ_H13/V\kappa J\kappa 13$ (●), V_H13G12-$DJ_H13/V\kappa J\kappa 13$ (○), $V_HDJ_H13/V\kappa 13K20$-$J\kappa 13$ (△), and V_H13G12-$DJ_H13/V\kappa 13K20$-$J\kappa 13$ (Δ) IgC1 Abs to solid-phase insulin by increasing amounts of soluble insulin. Vertical bars depict standard deviations.

Table I

Sequences of the oligonucleotide primers used for the construction of recombinant Ig V genes[a]

Leader-mAB13V_H-D-J_H gene segment	
H-leader (sense)	5′ gggaagcttctcaccatgggatgg 3′
H-FR4 (antisense)	5′ gggctcgagactcaccTGAGGAGACAGTGACCA 3′
H-Ov1 (antisense)	5′ GCTGCACCTCacactggacacctgcagagaaag 3′
H-Ov2 (sense)	5′ ttctctgcaggtgtccagtgtGAGGTGCAGCTG 3′
Leader-mAb13Vκ-Jκ gene segment	
κ-leader (sense)	5′ gggaagcttatcaagatgaagtca 3′
κ-FR4 (antisense)	5′ gggctcgagacttacgTTTGATCTCCACCTTGG 3′
κ-Ov1 (antisense)	5′ CAACACAATTTCgcatctggaacctgcagtcagaga 3′
κ-Ov2 (sense)	5′ gcaggttccagatgcGAAATTGTGTTGACGCAGTCT 3′
Recombination of germline and mutated V gene segments	
GIII-FR3 A (sense)	5′ GCAATGAACAGTCTGAGAGCCG 3′
GIII-FR3 B (antisense)	5′ CGGCTCTCAGACTGTTCATTGC 3′
13-FR2 A (sense)	5′ CCAGGGAAGGGGCTGGTGTGGGTCTC 3′
13-FR2 B (antisense)	5′ GAGACCCACACCAGCCCCTTCCCTGG 3′
κIII-FR3 A (sense)	5′ GAAGATTTTGCAGTGTATTACTGTCAGC 3′
κIII-FR3 B (antisense)	5′ GCTGACAGTAATACACTGCAAAATCTTC 3′
Mutagenized primers	
Thr56 A (sense)	5′ GGGAGT*ACC*ACAAGCTACGCGG 3′
Thr56 B (antisense)	5′ CCGCGTAGCTTG*TGG*TACTCCC 3′
Arg58 A (sense)	5′ GGGAGTAGCACA*AGG*TACGCGG 3′
Arg58 B (antisense)	5′ CCGCGTA*CCT*TGTGCTACTCCC 3′

[a]Capital letters denote the sequences derived from the Ig V gene sequence of mAb13. Small letters denote the sequences derived from the expression vectors. Sequences of restriction sites are underlined. Codons of replacement mutations in the mutagenesis primers are indicated by underlined italic letters.

Table II

Identity of the sequences of the 10 autologous germ-line VκIII genes to those of the germ-line kv3g, kv3g″, and kv325 genes, and to the sequence of mAb13 Vκ gene segment

	Heterologous Germ-line Genes (% Identity)[b]			
Autologous Germ-line Genes[a]	**kv3g**	**kv3″**	**kv325**	**mAb13, Vκ Segment**
13K20, 13K23	100[c]	98.6	95.5	97.3
13K11, 13K12	98.6	100	95.0	95.9
13K07, 13K09	98.2	99.4	96.4	95.4
13K04	97.3	96.3	95.0	94.5
13K18	95.5	95.5	100	92.8
13K16, 13K17	93.2	92.8	96.4	90.5

[a] The 10 autologous germ-line VκIII genes were isolated from the PMN DNA of the IDDM patient whose B cells were used for the generation of mAb 13 (Casali et al., *J. Immunol.* 144:3741, 1990; Ikematsu et al., *J. Immunol.* 152:1430, 1994).

[b] The germ-line kv3g and kv3g″ genes were originally reported by Pech and Zachau (*Nucleic Acids Res.* 12:9292, 1984) as Vg and Vg″, respectively. The germ-line kv325 was originally reported by Kipps et al. (*Proc. Natl. Acad. Sci.* USA 84:2916, 1987).

[c] Percent of identity was calculated for the sequence spanning residues 22 to 243 (Fig. 3). Such sequence may (219 nucleotides in genes kv3g, kv3g″, 13K20/13K23, 13K11/13K12, 13K07/13K09) or may not (222 nucleotides in genes kv325, 13K16/13K17, 13K18) include the AGC triplet deletion in the CDR1 (Fig. 3).

Table III

Binding of insulin by different recombinant IgG1 consisting of the "wild type" VκJκ chain and full or partial "germ-line revertant" V_H chains, as assessed by competitive inhibition and kinetic assays

	Segment Residues					Kinetic Analysis		
	CDR1	CDR2						
Recombinant IgG1	**31**	**52**	**56**	**58**	**Competitive Inhibition Av_{rel} (g/μl)**	**κ_{on} (10^4 M^{-1}·s^{-1})**	**κ_{off} (10^{-3} s^{-1})**	**K_d (nM)**
V_H13G12-DJ_H13/VκJκ13	S	N	S	S	1.44×10^{-8}	2.60	4.92	189
V_HDJ_H13/VκJκ13	G	—	T	RE	4.91×10^{-9}	2.73	1.35	49
Gly31/VκJκ13	G	—	—	—	1.62×10^{-8}	2.98	4.35	148
Thr56, Arg58/VκJκ13	—	—	T	R	4.62×10^{-9}	2.91	1.12	38
Thr56/VκJκ13	—	—	T	—	1.87×10^{-8}	2.56	4.22	164
Arg58/VκJκ13	—	—	—	R	5.14×10^{-9}	2.61	1.54	59
Lys52/VκJκ13	—	K	—	—	No binding	ND	ND	ND